Appl Compos Mater (2010) 17:621–637
DOI 10.1007/s10443-010-9132-4

Tailoring Sandwich Face/Core Interfaces for Improved Damage Tolerance—Part II: Experiments

Christian Lundsgaard-Larsen · Christian Berggreen · Leif A. Carlsson

Received: 10 January 2010 / Accepted: 14 March 2010 / Published online: 30 April 2010

Abstract A face/core debond in a sandwich structure may propagate in the interface or kink into either the face or core. It is found that certain modifications of the face/core interface region influence the kinking behavior, which is studied experimentally in the present paper. A sandwich double cantilever beam specimen loaded by uneven bending moments (DCB-UBM) allows for accurate measurements of the J integral as the crack propagates under large scale fibre bridging. By altering the mode-mixity of the loading, the crack path changes and deflects from the interface into the adjacent face or core. The transition points where the crack kinks are identified and the influence of four various interface design modifications on the propagation path and fracture resistance are investigated.

Keywords Sandwich structure · Fibre bridging · J integral · DCB-UBM · Crack kinking

1 Introduction

Composite structures often contain weak planes between layers allowing delaminations in monolithic composites or debonds in sandwich composites to form during production or service. Depending on the flaw size and loading configuration a

C. Lundsgaard-Larsen · C. Berggreen (✉)
Department of Mechanical Engineering, Technical University of Denmark,
2800 Lyngby, Denmark
e-mail: cbe@mek.dtu.dk

L. A. Carlsson
Department of Mechanical Engineering, Florida Atlantic University,
Boca Raton, FL 33431, USA

debond in a sandwich structure can act as a starter crack that may spread in a stable or unstable manner throughout large parts of the structure. Composite materials are often heterogeneous and anisotropic, and failure modes vary significantly from the ones in isotropic materials. To take full advantage of the high potential composites have to offer, it is necessary to increase knowledge about failure modes and damage tolerance.

This study mainly focuses on sandwich structures with two glass fibre/polyester faces separated by a foam core. Debonds may occur between face and core, thus it is important to maximize the fracture resistance of the interface to prevent the crack from propagating. The aim of the present paper is to investigate how various modifications of a face/core sandwich interface may influence the crack propagation behaviour and thus improve the fracture resistance of an interface crack. This paper constitutes part II in a series of two papers where part I describes various concepts to modify the interface and a finite element analysis of the test specimen. The present paper (part II) is concerned with the experimental investigation.

2 Tailoring the Face/Core Interface

As described in Part I [1] a face/core interface crack in a sandwich structure may propagate in three basic ways: (1) self similar in the interface, (2) kink into the core or (3) kink into the face. The actual path depends on the fracture resistances of the face, core and interface and the mode-mixity of the applied loading. The crack tends to propagate where the resistance is the least, so that e.g. a tough interface combined with a brittle core may result in crack kinking and propagation into the core regardless of the applied mode-mixity. It is thus necessary to tailor the sandwich interface according to the fracture properties of the face, core and interface, and to the in-service mode-mixity loading regime.

In some applications crack kinking into and propagation through the face laminate is desired, since then the critical crack will disappear from the structure. For other structures a scenario where the crack kinks into the face laminate is critical, since this may severely damage the load carrying laminate. In this case it is preferred if the crack is contained by a sufficiently tough interface, without kinking into the adjacent face or core. It may be possible to influence the crack path by e.g. inserting a thin tough layer adjacent to the load carrying laminate which the crack cannot penetrate, hereby restricting crack kinking into the laminate. Regardless of the preferred scenario, it is an aim to be able to influence the crack kinking behaviour by modifying the sandwich interface. This will be studied experimentally in this paper.

A few previous studies describes methods for stopping a sandwich interface crack. In [2] the crack is removed from the structure by leading the crack through the sandwich face hereby releasing the debonded panel. In [3] the crack is successfully stopped by inserting a wedge-shaped profile in the core during manufacturing, which will deflect the crack from the interface and arrest the crack in the crack stopper profile. In [4] a cylindrical shape is inserted into the core which suppresses the energy release rate as the crack approaches the inserted profile. All three crack stoppers rely on the assumption that the crack will travel in the core or face/core interface. In the present study it is an aim to make it attractive for the crack to propagate in

the interface, even for very light core materials, and propagate with a relative high fracture resistance due to the aid of bridging fibres.

In several sandwich applications a mat with randomly oriented fibres, i.e. chopped strand mat (CSM) is inserted between the face and core. The purposes of this mat are: (1) to increase the resin flow near the core during production and thus avoid any resin starved "dry" areas, (2) obtain a more gradually changing stiffness from the compliant core to the stiff face, and (3) toughening by fibre bridging (fibre bridging is increased since fibre bundles are relatively easily being pulled out of the mat).

In an experimental study Cantwell and Davies [5] prepared sandwich specimens with and without a CSM inserted in the face/core interface were compared for sandwich beams with GFRP faces and balsa cores. For the interface without CSM the crack propagated in the face/core interface, whereas for the specimen with CSM the crack propagated within the CSM layer with an energy release rate 30 % lower than the specimens without CSM. Cantwell [6] applied a CFM at the face/core interface of sandwich specimens with glassfibre/vinylester faces and either balsa or H200 foam core. The CFM layer generated a resin-rich layer where the crack propagated with large-scale bridging. Approximately the same fracture toughness was obtained as for the reference specimens without CFM.

A hypothetical example of a sandwich with a brittle foam core is considered in the following to illustrate the correlation between fracture toughness and crack kinking and how the damage tolerance may be maximized. For the interface without CSM, see Fig. 1a, $J_o^{core} < J_o^{face}$ and it is likely that the crack will propagate in the core, with the energy release rate equal to J_o^{core} (since the process zone in the core is small $J_{ss}^{core} \simeq J_o^{core}$). For the interface with CSM illustrated in Fig. 1b, $J_o^{CSM} < J_o^{core}$ it is

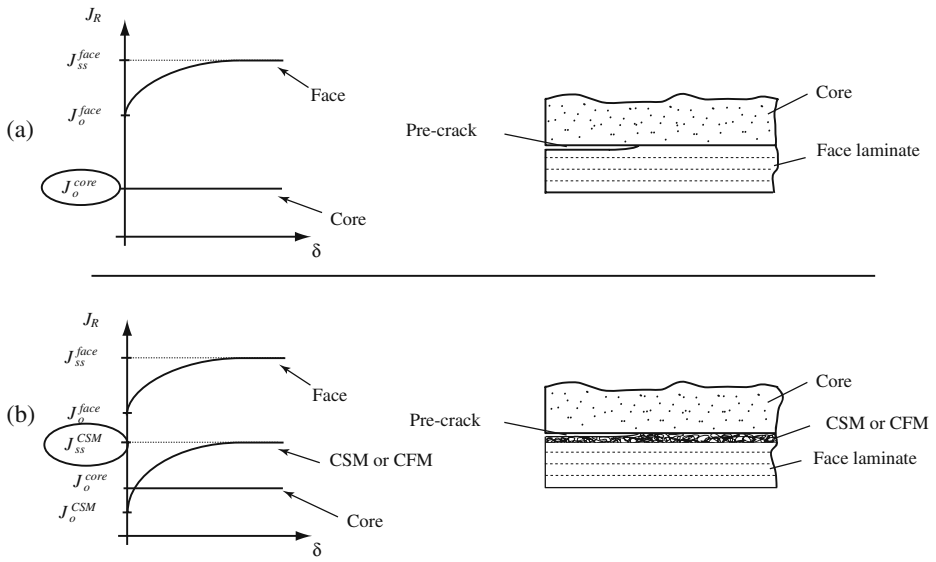

Fig. 1 Hypothetical fracture resistance curves for **a** interface without CSM and **b** interface with CSM. The steady state fracture toughness is equal to the crack driving force necessary to propagate the crack when the process zone has evolved

likely that the crack propagation will start in the CSM layer. However, this growth will produce large scale fibre bridging and the total fracture resistance increases to $J_{ss}^{CSM} > J_{o}^{core}$. Unless the crack kinks into the core it will remain in the CSM layer. The optimal interface layer for increasing the fracture resistance while avoiding crack kinking, is therefore one where the crack tip toughness is relatively small whereas the energy dissipation in the crack wake behind the crack tip should be relatively large.

3 Materials and Specimen Geometry

In this section the specimen configuration and loading as well as the process of manufacturing the specimens are described along with modifications implemented to influence the crack kinking behavior.

The DCB-UBM test rig allows loading of sandwich specimens by edge moments. A schematic illustration of the test rig and the loaded sandwich specimen is shown in Fig. 2, whereas a more detailed description can be found in [7].

The moments, M_1 and M_2 acting on the legs of the DCB specimen, are obtained from a roller-wire system connected to the top edges of the specimen. The moments are determined from the wire tension, P, and the distances, l_1 and l_2, between the rollers, see Fig. 2,

$$\begin{aligned} M_1 &= Pl_1 \\ M_2 &= Pl_2 \end{aligned} \tag{1}$$

Both moments defined positive counterclockwise. The ratio between M_1 and M_2 is adjusted by changing the distances, l_1 and l_2, between the rollers. Furthermore, the direction of the moments can be reversed by changing the mounting direction of the wire. If moments with opposite signs are applied, e.g. $M_1/M_2 = -1$, crack opening in the normal direction is dominating (mode I). If moments with the same

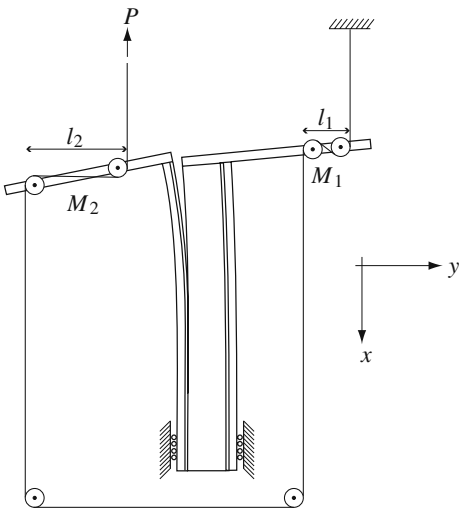

Fig. 2 Schematic of the loading principle of a DCB-UBM sandwich specimen

sign are applied, the crack sliding in the tangential direction is dominating (mode II). To limit deflections and rotations of the beams the sandwich specimen was reinforced by bonding a 6 mm thick steel bar to each of the sandwich faces, see Fig. 3 and [8] for further details.

For the specimen utilized in this study, the J integral can be determined analytically from specimen geometry, elastic properties and applied moments by considering a contour along the outer boundaries of the specimen. This is described in Part I [1].

It is an aim to explore the possibility for designing an interface, where the crack will propagate with high degree of fibre bridging and thus potentially higher fracture toughness, without increasing the tendency for the crack to kink into (and damage) the load-carrying laminate. Specimens were manufactured with a reference lay-up containing a chopped strand mat (CSM) at the face/core interface, i.e. the specimen were made with the following lay-up: $DBLT850_4$, CSM450, H200 core, $DBLT850_4$. The DBLT850 mat manufactured by Devold Amt is quadraxial with a dry area weight of 850 g/m^2 and with fibre directions relative to the longitudinal direction of the specimen [90,45,0,−45], where the −45 degree ply is placed closest to the core. A CSM with an area density of 450 g/m^2 was inserted between the core and the quadraxial laminates during production and the total face thickness after production is approximately 2.9 mm.

In addition to the reference specimen, the following configurations were examined:

(1) The chopped strand mat (CSM) is substituted with a continuous filament mat (CFM), i.e. long fibre bundles instead of short.
(2) A thin woven glass fiber layer (a “kink stopper”) is placed at the interface to prevent crack kinking into the adjacent face laminate. The woven layer is inserted between the face and the CSM to create a mechanical “wall” with a relatively high in-plane toughness and strength which is difficult to penetrate.
(3) The face laminate is stitched with an aramid thread before production to sustain the face layers together hereby limiting the tendency for crack kinking into the load-carrying laminate and for secondary cracks to emerge above the kink stopper in the face sheet.
(4) Specimens with a H130 core are considered in order to investigate the influence of the core on the crack propagation behavior.
(5) The standard specimen is 30 mm wide, and the effect of altering this dimension is considered to examine the effect of specimen with on the measured fracture resistance.

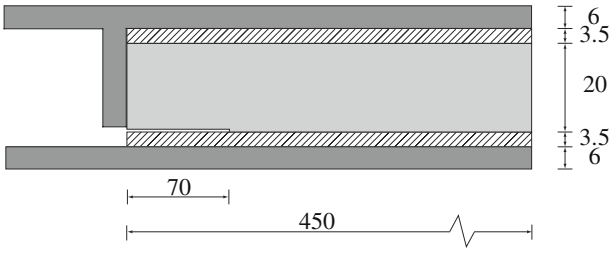

Fig. 3 Sandwich specimen with a 70 mm long pre-crack (dimensions in mm). The specimen is stiffened by 6 mm steel bars bonded to the faces

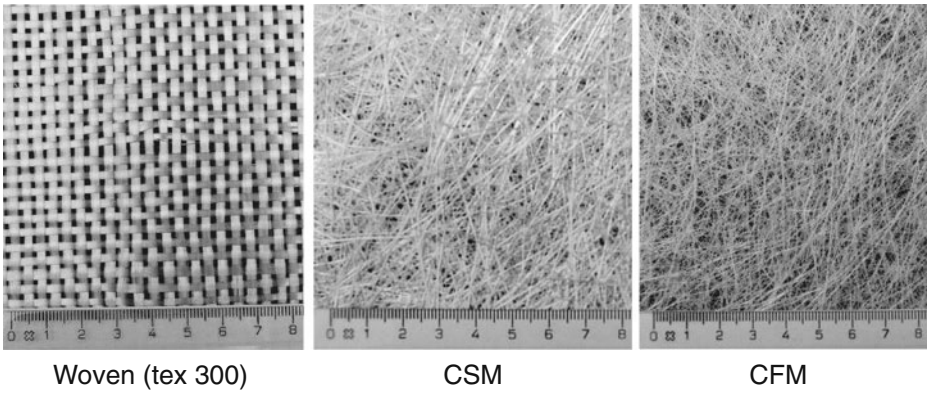

Fig. 4 Photos of various laminates used in this study (unit on ruler is cm)

The various modification are specified in more detail below.

(1) *Continuous filament mat (CFM) instead of CSM*
A continuous filament mat (CFM) consist of long (in principle continuous) randomly oriented fibre bundles, in contrast to the CSM mat where fibre bundles are 4–6 cm long. Even though the dry CSM and CFM mats have the same area density (450 g/m^2), the CFM layer is approximately 0.5 mm thicker, thus it constitutes a larger volume in its dry form. After the resin infusion process the resin replaces the excessive air and the extra thickness leads to a higher resin content compared to the CSM. Photos of the dry CSM and CFM mats can be seen in Fig. 4.

(2) *Woven layer as a crack stopper*
Preliminary tests indicate that the crack may kink into the adjacent laminate when the mode-mixity is sufficiently mode II. To restrict kinking, a plain weave of tex 300, Fig. 4, is inserted between the CSM/CFM and the multi-axial face sheet. The weave has a relatively high in-plane strength and fracture toughness, which should resist cracks that tend to kink into the adjacent laminate. The lay-up sequence of a sandwich interface with an additional woven mat is illustrated in Fig. 5.

(3) *Stitching*
Face laminates and a woven tex 300 layer were stitched with an aramid thread type 2300 from the manufacturer Teijin using basic stitches in the longitudinal direction see Fig. 6. The stitches are separated approximately 5 mm, and stitching is conducted with a thread force balanced to be high enough to constrain the laminate thoroughly, yet small enough to allow the laminate to

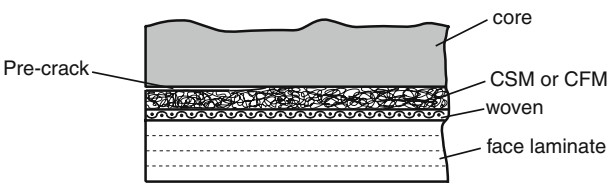

Fig. 5 Schematic illustration of lay-up sequence in tested sandwich interface

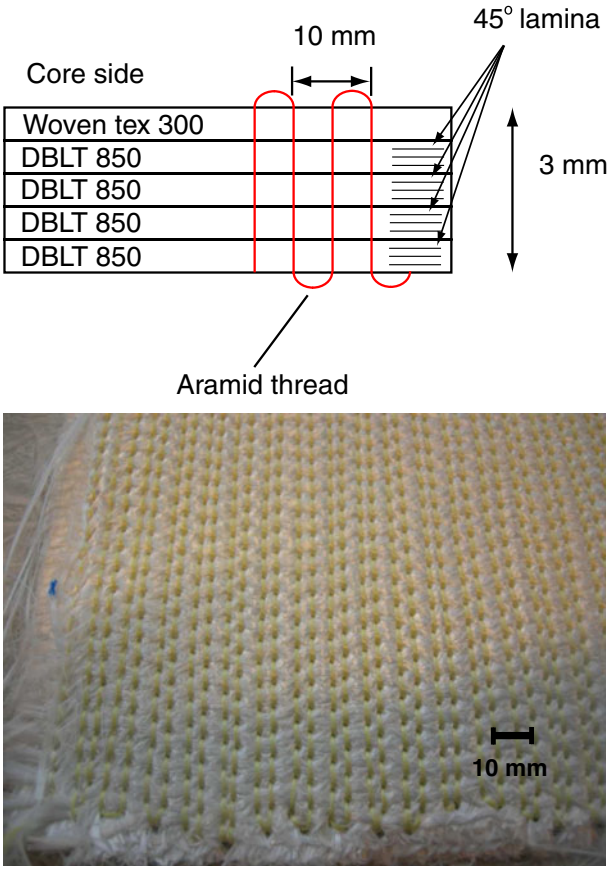

Fig. 6 A woven tex 300 laminat is stitched together with four DBLT850 mats using basic stitches

remain straight and flat after stitching. A photograph of the stitched laminate before vacuum injection is shown in Fig. 6.

(4) *Lighter core*

Two core materials were considered, Divinycell H130 and H200 from DIAB AB, with nominal densities of 130 and 200 kg/m^3 respectively. Both are cross-linked, closed cell PVC foams with mechanical properties given in the manufactures datasheet [9] and in Table 1.

Additional mode I fracture tests were conducted on the H130 and H200 core using a DCB-UBM specimen in order to determine the core fracture toughness. The tests were conducted by adhering 6 mm steel bars directly to the foam

Table 1 Elastic properties of the core materials

Property	Value
H130 Young's modulus	170 MPa
H130 Poisson's ratio	0.29
H200 Young's modulus	250 MPa
H200 Poisson's ratio	0.29

material and applying a 60 mm pre-crack cut with a 1 mm saw blade in the middle of the core specimen.

(5) *Specimen width*
The width of the standard specimen is 30 mm and it is investigated whether changing this dimension may have an influence on the results. As the crack propagates in the CSM or CFM layer the amount of fibre bridging may depend on the length of the fibres able to bridge the crack. As the sandwich panel is cut into narrow specimens the average length of fibres in the CSM or CFM mat is reduced significantly, which may influence the steady-state fracture resistance as the crack propagates under large-scale bridging. To investigate the influence of the width, specimens of 20, 30 and 40 mm were manufactured for the reference and the CFM cases.

Sandwich panels with glass fibre faces and foam cores were manufactured using resin vacuum infusion, and a 70 mm wide 12.5 μm thick slip film was inserted between part of the face and core to define the pre-crack. The polyester resin Polylite® 413-575 is specially suitable for vacuum infusion due to its low viscosity (Fig. 7).

During the resin infusion process a vacuum of 0.1 bar was maintained inside the bag and subsequently the panel was cured at room temperature for 16 h with an internal vacuum of 0.6 bar. The panel was then unwrapped and post-cured in an oven for 24 h at a temperature of 60°C.

Test matrix is provided in Table 2. The sandwich specimens were loaded by pure bending moments applied at the end of the specimen. Details regarding the test-rig and loading principle are thoroughly described in [7] and a procedure for evaluating the J integral is presented in Part I [1]. Prior to conducting the test a speckled pattern is applied to the specimen surface by using first white and then black spray paint. The speckled pattern allows the tracking of full field displacements using a commercial digital image correlation (DIC) system, ARAMIS 2M manufactured by GOM.

Since the fracture behaviour of the specimens is not known a priori, the choice of moment ratio M_1/M_2 (and consequently mode-mixity) was made progressively as the tests were conducted according to the observed fracture behavior.

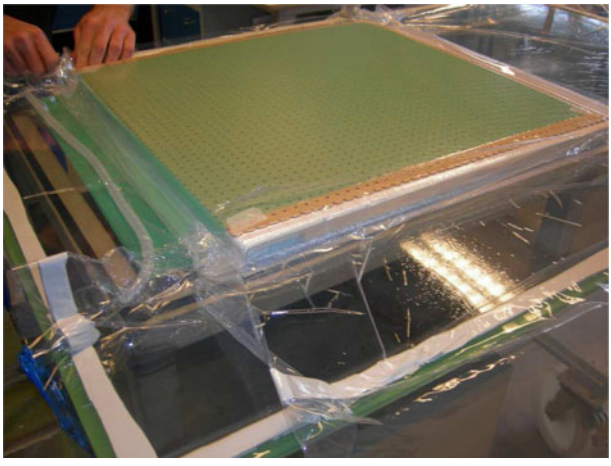

Fig. 7 During the resin infusion process the glass-fiber mats are placed on a table with resin inlet on one side of the sandwich panel and vacuum suction on the opposite side

Table 2 Test matrix for a total of 83 specimens; number of replicates, core type, interface lay-up, moment ratios, and corresponding average mode-mixity m_{avg} and crack tip mode-mixity m_{tip} are found from simulation of the DCB-UBM specimen, see [1]

Replicates	Core	Layer	M_1/M_2	m_{avg}	m_{tip}
3^r	H200	CSM	−0.5	0.013	0.14
$3^{r,w}$	H200	CSM	0.0	0.23	0.64
3^r	H200	CSM	0.2	0.39	0.98
3	H200	CFM	−0.5	0.013	0.14
3	H200	CFM	−0.2	0.13	0.39
3^w	H200	CFM	0.0	0.23	0.64
3	H200	CFM	0.15	0.35	0.84
3	H200	CSM + tex 300	−0.4	0.043	0.21
3	H200	CSM + tex 300	−0.2	0.14	0.31
3	H200	CSM + tex 300	−0.12	0.18	0.37
3	H200	CSM + tex 300	0.0	0.24	0.43
3	H200	CSM + tex 300	0.2	0.36	0.55
1	H200	CSM + tex 300	0.3	0.42	0.60
2	H200	CFM + tex 300	−0.4	0.043	0.21
3	H200	CFM + tex 300	−0.3	0.087	0.26
3	H200	CFM + tex 300	−0.12	0.18	0.37
3	H200	CFM + tex 300	0.0	0.24	0.43
3	H200	CFM + tex 300	0.15	0.33	0.53
4^s	H200	CFM + tex 300	0.0	0.24	0.43
3^s	H200	CFM + tex 300	0.15	0.33	0.53
3^s	H200	CFM + tex 300	0.3	0.68	0.99
3^s	H200	CFM + tex 300	0.5	0.80	1.0
3^s	H130	CFM + tex 300	−0.5	0.0028	0.16
4^s	H130	CFM + tex 300	−0.3	0.087	0.26
3^s	H130	CFM + tex 300	−0.12	0.18	0.37
3^s	H130	CFM + tex 300	0.0	0.24	0.43
3	H130	–	−1	0	0
3	H200	–	−1	0	0

The following superscripts are used: "r" marks the reference specimens, "w" indicates that the test is repeated for 20 and 40 mm specimens to explore the influence of specimen width and "s" entails that the face laminate is stitched

4 Results and Discussion

This section is organized into five subsections: General observations, Effect of the woven layer, Effect of stitched face sheets, Specimen with lighter core, and Effect of specimen width.

4.1 General Observations

Full-field displacement measurements are recorded by the DIC system, and the opening displacement of the pre-crack tip is extracted from the measurements and separated into normal and tangential components δ_n and δ_t, see [8]. Figure 8 shows an example of the J integral value plotted as function of the effective pre-crack tip displacement $\delta^* = \sqrt{\delta_n^2 + \delta_t^2}$. Initially J increases rapidly, with only very small opening of the pre-crack tip. As the J integral value exceeds the fracture toughness of the material, the crack propagates and the pre-crack tip opens. Bridging fibres connect the separating faces, see Fig. 9, and as a result the fracture resistance increases and a larger J integral value is needed to propagate the crack. Assuming that the specimen is loaded monotonically with constant mode-mixity the process zone

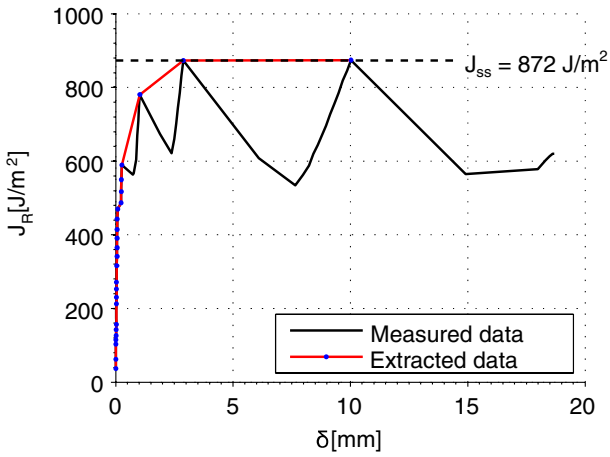

Fig. 8 Measured and extracted data (J_R vs. opening at the pre-crack tip location) from a reference DCB-UBM test with $M_1/M_2 = 0$

eventually reaches a steady-state condition where the fracture resistance reaches a plateau, as indicated in Fig. 8.

It is observed from the tests that often the crack does not propagate in a stable manner, but in increments of 3–5 cm, resulting in the drops in J as observed in Fig. 8. Since the J integral is not affected by crack length, the observed unstable crack growth is caused by either material variations along the interface, or rate dependent fracture properties. As discussed in [10] plastic deformation tends to blunt the crack tip during load build-up leading to an increased static fracture resistance. As the pre-crack starts propagating the crack tip becomes sharp and less energy is needed to propagate the crack. Consequently, as the crack propagates more elastic energy is released than what is consumed propagating the crack, which leads to unstable (rapid) crack growth. The extent of the process zone length in a cracked specimen with large scale fibre bridging is illustrated in Fig. 9.

As mentioned previously, the crack may propagate in three basic ways: (1) the crack stays in the face/core interface e.g. with fibre pull-out of the CSM or CFM layer, (2) the crack kinks into the core or (3) the crack kinks into the face. For the materials used in the reference specimen all three regimes can be obtained by varying

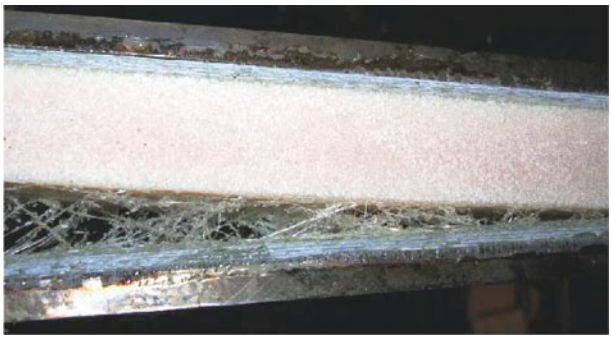

Fig. 9 A DCB-UBM specimen with a CFM layer loaded at a crack-tip mode-mixity of $m_{tip} = 0.39$. A crack is propagating in the CFM layer under large-scale bridging

the moment ratio M_1/M_2. In the cases where the crack kinked into the laminate, the crack gradually jumped from one layer to the next, and the distance (in the crack propagation direction) between points where the crack changed layer varied between 2 and 10 cm, decreasing with increasing m_{tip}. A picture of a reference specimen with a crack gradually kinking through the laminate is seen in Fig. 10. The crack initially propagated in the resin between the CSM and the core for 2–3 cm, then in the CSM, then in the $-45°$ layer and finally in the $0°$ layer. The $0°$ layer was not penetrated but for some specimens the crack continued on the other side of the $0°$ layer, thus generating a second crack tip. A schematic illustration of the crack path is shown at the bottom of Fig. 10.

The steady-state fracture resistance J_{ss} as a function of crack-tip mode-mixity is plotted in Fig. 11 for the following cases: a) CSM (reference case), b) CFM, c) CSM + woven, d) CFM + woven. In Fig. 11 the symbol "x" is used to mark results where the crack propagated in the CSM or CFM layer, the symbol "o" indicates that the crack kinked into the face, and the symbol "△" indicates crack kinking into the core. The approximate transition where the crack starts to kink into the adjacent face (quadraxial layers) is marked with a vertical dashed line.

For the reference specimen with CSM layer, Fig. 11a, three crack-tip mode-mixities were considered, $m_{tip} = \{0.14, 0.64, 0.79\}$. For two out of four specimens loaded by the mode-mixity $m_{tip} = 0.79$, the crack kinked into the face, whereas in all

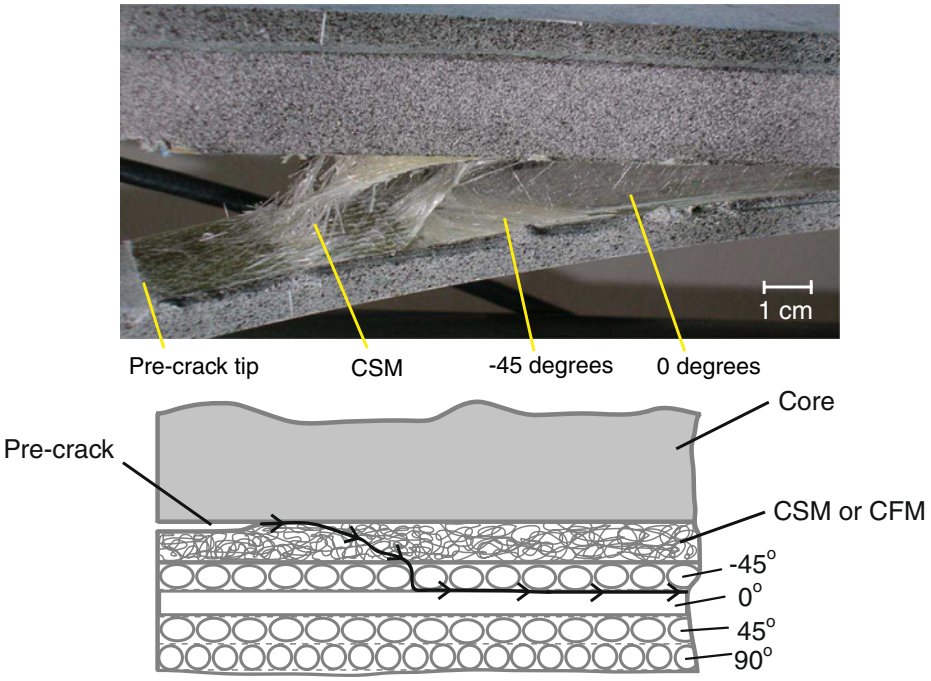

Fig. 10 Photo (*top*) and schematic illustration (*bottom*) of the crack propagation path in a reference DCB-UBM specimen with a CSM mat in the interface. The crack was gradually kinking through the CSM and face layers. The moment ratio is $M_1/M_2 = 0.2$ and $m_{tip} = 0.98$

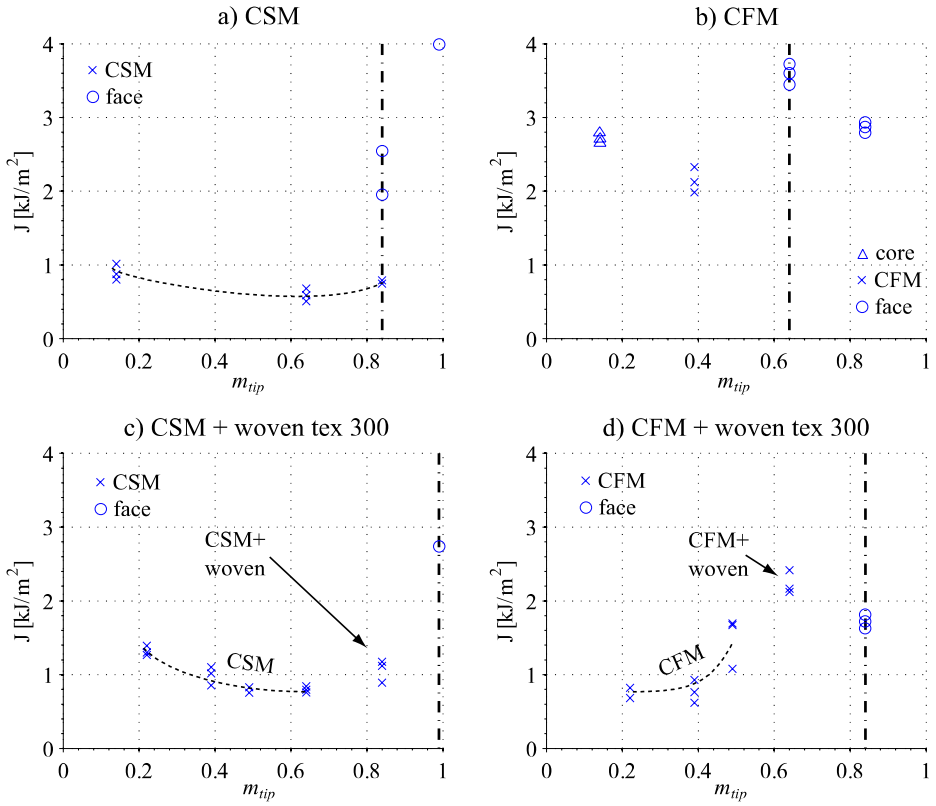

Fig. 11 Steady-state fracture resistance as a function of mode-mixity for sandwich specimens. The *x-symbol* indicates either crack propagation in the CSM or CFM layer or between the woven layer and the CSM or CFM, the *o-symbol* represents crack kinking into the face, and the △*-symbol* indicates crack kinking into the core. The *vertical dashed line* indicates the approximate transition where the crack kinked into the face

other cases the crack stayed in the CSM layer. As the crack kinked into the face, the measured fracture resistance increased substantially. The results for the CFM layer are shown in Fig. 11b, with the crack-tip mode-mixities $m_{tip} = \{0.14, 0.39, 0.64, 0.84\}$. In contrast to the specimens with CSM, a mode-mixity of $m_{tip} = 0.14$ led to crack kinking into the core, with a measured fracture toughness of approximately 2.7 kJ/m^2, which approximately corresponds to the measured mode I fracture toughness of the pure H200 core material (2.5 kJ/m^2). At a mode-mixity of $m_{tip} = 0.39$ the crack propagated in the CFM layer with large-scale bridging and a steady state fracture resistance between 2.0 and 2.3 kJ/m^2. For the final two crack-tip mode-mixities ($m_{tip} = 0.64$ and 0.84) the crack kinked into the face laminate, which entails increased fracture resistance compared to crack propagation in the CFM layer. The reason for the increased fracture resistance as the crack kinks into the quadraxial layers is probably that the crack crosses over a large number of fibers as it changes path.

The main idea in the present study behind inserting a CSM or CFM layer is to generate a source for fiber bridging hereby increasing the fracture resistance and damage tolerance. When comparing the performance of the two layers, fiber bundles seem easier to pull out of a CSM, since they are shorter than the CFM. This entails that the crack stays in the CSM layer at a larger mode-mixity interval, see Fig. 11 and that fiber bridging is more easily triggered. Conversely, the CFM layer has larger toughening potential if the crack grows within the CFM at the proper mode-mixity loading, since a CFM is resin rich and fibers are very long. Thus, the choice on CSM or CFM depends on the mode-mixity at the crack-tip.

4.2 Effect of the Woven Layer

The effect of a woven layer on the tendency for crack kinking into the adjacent quadraxial face is examined in this section. For the CSM + woven in Fig. 11c, specimens were tested at $m_{tip} = \{0.22, 0.39, 0.49, 0.64, 0.84, 0.99\}$ and only the mode-mixity of 0.99 showed kinking into the face. At a mode I dominated loading ($m_{tip} \simeq 0.22$), the crack propagated in the centre of the CSM, resulting in relatively dense fibre bridging, whereas a mode-mixity of $m_{tip} \simeq 0.64$ made the crack propagate in the outer region of the CSM mat with resulting less fibre bridging and consequently less fracture resistance. The plot for the CFM + woven configuration shown in Fig. 11 d) illustrates a somewhat different behavior. Here a mode I dominated loading leads to crack propagation in the resin between the core and the CFM layer, and only at more mode II dominated loadings ($m_{tip} = \{0.39, 0.49, 0.64\}$) the crack kinks into the CFM layer, resulting in increased fibre bridging and fracture resistance. As the crack propagates in the centre of the CSM or CFM layer the steady state fracture resistance is 1.2–1.8 kJ/m^2, whereas it is only 0.8 kJ/m^2 when the crack propagates in the outer region of the layer (for both CSM + woven and CFM + woven configurations).

The woven layer is never penetrated by the crack and succeeds to some degree as a kink-stopper. However, for highly mode II dominated cases, a secondary crack is initiated on the opposite side of the woven layer, which continues to propagate in the interface between woven and quadraxial layers without breaking the woven mat, see Fig. 12. This behaviour is further described later.

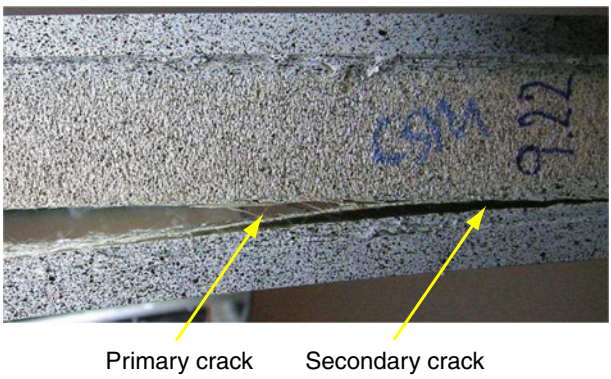

Fig. 12 A crack jumping to the opposite side of the woven layer without penetration, and thus initiating a second crack front. The specimen shown is CSM+woven layer loaded at $M_1/M_2 = 0.3$ which corresponds to a crack-tip mode-mixity of $m_{tip} = 0.84$

4.3 Effect of Stitched Face Sheets

It is believed that stitching the face may prevent delamination between layers, since the stitching thread retain laminate layers together and increases the separation resistance. To explore whether the stitches decrease the tendency for crack kinking and initiation of secondary crack fronts, the specimens are tested in a mode II dominated regime, where the non-stitched specimens showed crack kinking into the face laminate or initiation of secondary crack fronts for specimens with woven layers. The mode-mixities are $m_{tip} = \{0.64, 0.84, 0.99\}$ and the obtained J_{ss} values vs. mode-mixity are plotted in Fig. 13. It is found that the crack does not kink into the face laminate and no initiation of secondary crack fronts are observed as was seen for specimens with woven layers for any of the tested mode-mixities, thus stitching the laminate is shown to clearly reduce the tendency for crack kinking for the specimen configuration tested in this study.

The steady state fracture toughness value J_{ss} of the stitched laminate resembles that of the non-stitched laminate (approximately 2.2 kJ/m^2) when loaded by a crack-tip mode-mixity of $m_{tip} = 0.64$, see Figs. 11 and 13. For a mode II dominated loadings, i.e. $m_{tip} = 0.84$, the fracture toughness of the stitched CFM-woven laminate is $J_{ss} \approx 2.2$kJ/m^2 which is higher than for the non-stitched case ($J_{ss} \approx 1.8$kJ/m^2).

Stitching of the face laminate was shown to be the most effective method regarding prevention of crack kinking into the load carrying part of the laminate. For the stitched specimens considered in this study the crack did not kink into the load-carrying laminate even at highly mode II dominated mode-mixities. However, stitching has some disadvantages, which should be taken into consideration. Stitching is a rather slow and expensive process, especially for composite structures with a low cost per weight of material. Furthermore, stitching may damage or misalign fibers in the laminate, which may be critical especially during fatigue loading. Thus, the concept needs more detailed investigation in this respect. Finally, instead of stitching only the sandwich face another option could be to stitch through the entire sandwich panel.

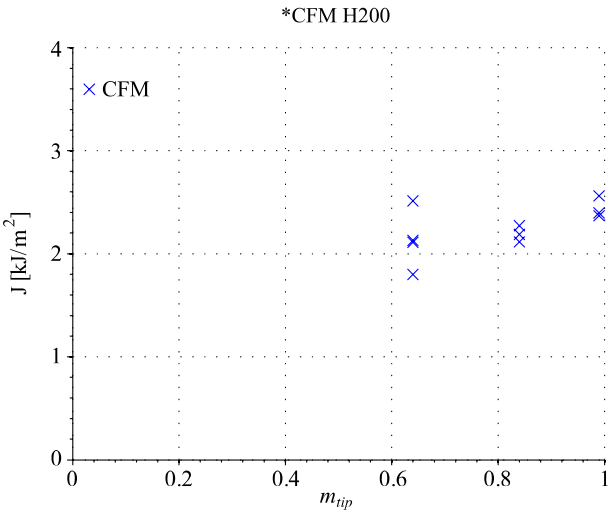

Fig. 13 Steady state fracture resistance as a function of mode-mixity for tested sandwich specimens, with a H200 core and stitched face laminate. For all specimens with a stitched face laminate the crack propagated in the CFM/woven interface

This would likely increase the fracture resistance and thus the damage tolerance of the face/core interface.

4.4 Specimens with Lighter Core

Specimens with a lighter and less tough core (H130 instead of H200) were tested. According to [11] and [12] the crack-tip mode-mixity transition should change as the fracture resistance and strength of the adjacent core is changed. Specimens with a H130 core, CFM layer, stitched and with no additional woven layer were tested at crack-tip mode-mixities $m_{tip} = \{0.14, 0.28, 0.49, 0.64\}$ and results are illustrated in Fig. 14. It was found that for all three repeated tests of the mode-mixity $m_{tip} = 0.28$ the crack kinked into the H130 core while, for the H200 case the crack propagated in the CFM layer at this mode-mixity, see Fig. 11. Thus the crack-tip mode-mixity transition point has moved from 0.39 to 0.49. The fracture resistance of the H130 core is measured to an average of 1.5 kJ/m^2, whereas the H200 was found to be approximately 2.5 kJ/m^2.

The mode I fracture toughness of the Divinycell H200 foam core is measured from the DCB-UBM experiments to 2.5 kJ/m^2, whereas [13] measured a fracture toughness of 1.3 kJ/m^2 for H200 core material. However, through correspondence with the manufacturer of the core material it has been clarified that since the paper by [13] was published, the material formulation for the entire H-series PVC cores has been altered, and the fracture toughness improved. This is believed to be the cause for the relatively large difference between the two measured fracture toughness values.

The scenario where the crack kinks into the adjacent core is not treated thoroughly in this study. However, it is found that the fracture toughness of the pure H130 and H200 core materials ($J_{core} = 1.5$ kJ/m^2 and $J_{core} = 2.5$ kJ/m^2 respectively) are relatively high compared with the steady state fracture resistance of the CSM or CFM layer (between 0.8 and 2.4 kJ/m^2). Therefore crack propagation in the core material might lead to superior fracture resistance compared to the CSM or CFM

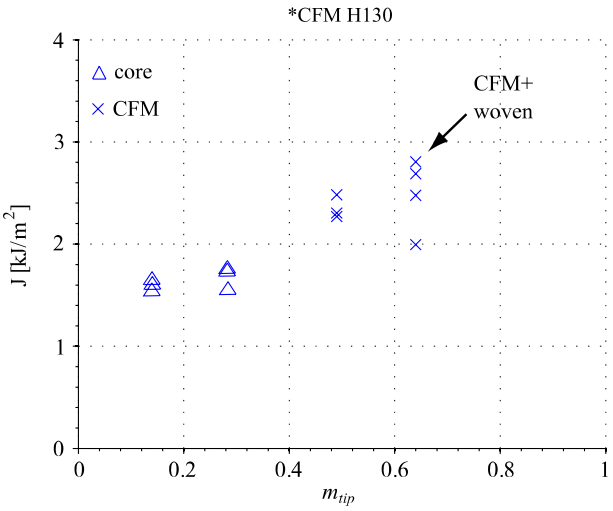

Fig. 14 Steady-state fracture resistance as a function of mode-mixity for sandwich specimens with a H130 core and stitched face laminate

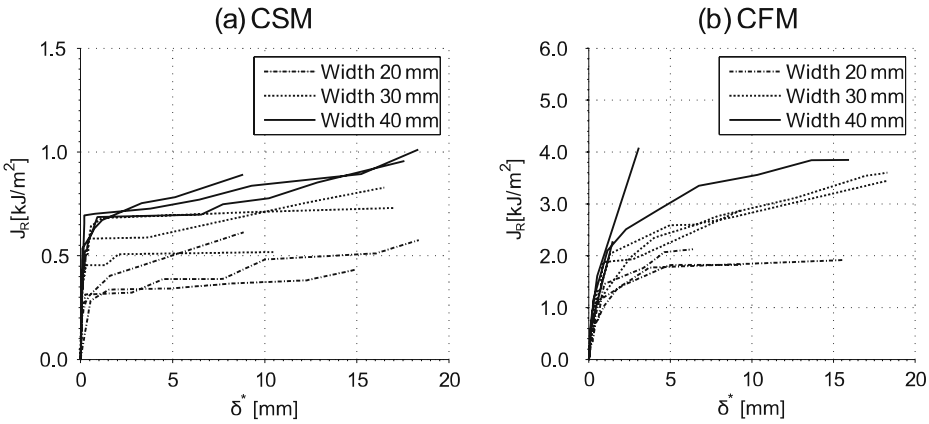

Fig. 15 Fracture resistance J_R as function of opening displacement δ^* for specimens of 20, 30 or 40 mm widths. Subplot **a** shows results for specimens with a CSM layer in the interface, and **b** results for a CFM in the interface. No additional woven layer is present. Both are loaded with the moment ratio $M_1/M_2 = 0$

layers. By comparing the crack kinking behaviour of specimens with an H130 core with H200, it is found that the tendency toward crack kinking into the core increases with decreasing core density. This behaviour is expected and in agreement with earlier studies in the literature [14] and with crack kinking studies mentioned in the introduction. From a damage tolerance and fracture prediction point of view, it is desired to investigate the crack-tip mode-mixity transition where the crack will kink into the core, and the consequent energy release rate as the crack propagates in the core (similar to what is conducted in this study).

4.5 Effect of Specimen Width

The effect of specimen width is investigated. The test specimens were either CSM or CFM non-stitched and without any woven layer. J_R vs. δ^* results for specimens of 20, 30 and 40 mm widths are displayed in Fig. 15.

It is seen that for both CSM and CFM cases the measured fracture resistance increases with increasing width. In the presence of large scale bridging, fibres will cross the crack in different angles including across the width direction, which suggests that the width dimension might have an influence on the fracture toughness, especially if the width is less than the fiber length. This is not investigated further in the present paper.

5 Conclusions

Various concepts to prevent crack kinking into the face and enhance the face/core fracture resistance have been examined experimentally. Such concepts are the use of a chopped strand mat (CSM) or a continues filament mat (CFM) between face and core, a layer of woven fabric between the face and CSM, and stitching of the layers of the face laminate. In addition, the effects of core material and specimen width were

examined. The highest overall toughness was achieved with the CFM layer, although kinking into the face occurred at relatively low mode mixity. It was found that the mode mixity range where the crack propagated in the face/core interface region could be extended by the woven fabric layer placed adjacent to the face. Stitching was found to prevent kinking of the crack into the face layers and provide overall high toughness. The specimens with a lower density core (H130) failed by crack kinking into the core at low mode mixities. Overall the debond toughness was much less than for the H200 core. The fracture toughness increased with specimen width as a result of more bridging fibers participating in the fracture process.

Acknowledgements This work has been partially performed within the context of the research project "Growth of Debonds in Foam Cored Sandwich Structures under Cyclic Loading" (SANTIGUE) funded by the Danish Research Agency (Grant No. 274-05-0324), and partially within the Network of Excellence on Marine Structures (MARSTRUCT) partially funded by the European Union through the Growth Programme under contract TNE3-CT-2003-506141. Furthermore, the supply of core materials from DIAB, borrowing of the DCB-UBM test rig from Risø DTU and the support from the Otto MønstedŠs Foundation for a guest professorship for Leif A. Carlsson at the Technical University of Denmark are likewise highly appreciated.

References

1. Lundsgaard-Larsen, C., Berggreen, C., Carlsson, L.A.: Tailoring sandwich face/core interfaces for improved damage tolerance—part I: finite element analysis. Appl. Compos. Mater. (2010). doi:10.1007/s10443-010-9131-5
2. Wonderly, C., Grenestedt, J.: Dynamic performance of a peel stopper for composite sandwich ship structures. J. Compos. Mater. **38**(10), 805–831 (2004)
3. Jakobsen, J., Bozhevolnaya, E., Thomsen, O.T.: New peel stopper concept for sandwich structures. Compos. Sci. Technol. **67**(15–16), 3378–3385 (2007)
4. Hirose, Y., Hojo, M., Fujiyoshi, A., Matsubara, G.: Suppression of interfacial crack for foam core sandwich panel with crack arrester. Adv. Compos. Mater.: Official J. Jpn. Soc. Compos. Mater. **16**(1), 11–30 (2007)
5. Cantwell, W.J., Davies, P.: A study of skin-core adhesion in glass fibre reinforced sandwich materials. Appl. Compos. Mater. **3**(6), 407–420 (1996)
6. Truxel, A., Aviles, F., Carlsson, L.A., Grenestedt, J.L., Millay, K.: Influence of face/core interface on debond toughness of foam and balsa cored sandwich. J. Sandw. Struct. Mater. **8**, 237 (2006)
7. Sørensen, B.F., Jørgensen, K., Jacobsen, T.K., Østergaard, R.C.: DCB-specimen loaded with uneven bending moments. Int. J. Fract. **141**(1), 163–176 (2006)
8. Lundsgaard-Larsen, C., Sørensen, B.F., Berggreen, C., Østergaard, R.C.: A modified DCB sandwich specimen for measuring mixed-mode cohesive laws. Eng. Fract. Mech. **75**(8), 2514–2530 (2008)
9. DIAB: www.diabgroup.com. Accessed June 2008
10. Kinloch, A.J., Williams, J.G.: Crack blunting mechanisms in polymers. J. Mater. Sci. **15**(4), 987–96 (1980)
11. Suo, Z., Hutchinson, J.W.: Interface crack between two elastic layers. Int. J. Fract. **43**(1), 1–18 (1990)
12. Parmigiani, J.P., Thouless, M.D.: The roles of toughness and cohesive strength on crack deflection at interfaces. J. Mech. Phys. Solids **54**(2), 266–287 (2006)
13. Viana, G.M., Carlsson, L.A.: Influences of foam density and core thickness on debond toughness of sandwich specimens with PVC foam core. J. Sandw. Struct. Mater. **5**, 103 (2003)
14. Berggreen, C., Simonsen, B.C., Borum, K.K.: Experimental and numerical study of interface crack propagation in foam-cored sandwich beams. J. Compos. Mater. **41**(4), 493–520 (2007)